

Quasielastic scattering of ${}^9\text{Li}$ on ${}^{12}\text{C}$

M. Zahar, M. Belbot, J. J. Kolata, and K. Lamkin
Physics Department, University of Notre Dame, Notre Dame, Indiana 46556

D. J. Morrissey and B. M. Sherrill
National Superconducting Cyclotron Laboratory, Michigan State University, East Lansing, Michigan 48824

M. Lewitowicz
GANIL, BP 5027, F-14021, Caen, France

A. H. Wuosmaa
Physics Division, Argonne National Laboratory, Argonne, Illinois 60439

J. S. Al-Khalili, J. A. Tostevin, and I. J. Thompson
Department of Physics, University of Surrey, Guildford, Surrey GU2 5XH, United Kingdom
 (Received 31 January 1996)

The quasielastic scattering of ${}^9\text{Li}$ on a ${}^{12}\text{C}$ target has been measured at an incident energy of 540 MeV. The new experimental data are used to extract an effective interaction for ${}^9\text{Li} + {}^{12}\text{C}$ scattering. The uncertainty in this interaction was previously a major obstacle to extracting information on the structure of ${}^{11}\text{Li}$ from existing ${}^{11}\text{Li} + {}^{12}\text{C}$ quasielastic-scattering data. [S0556-2813(96)03309-2]

PACS number(s): 25.60.-t, 24.10.Ht, 25.70.Bc, 27.20.+n

I. INTRODUCTION

In a previous experiment [1], we investigated the quasielastic scattering of the exotic “two-neutron halo” nucleus ${}^{11}\text{Li}$ from a ${}^{12}\text{C}$ target. Subsequent theoretical calculations [2] of this scattering process using a four-body Glauber model confirmed, in principle, that a measurement of the elastic-scattering angular distribution can provide a useful indicator of the nature of the ${}^{11}\text{Li}$ ground state. These calculations clearly showed that the elastic-scattering data are sensitive to the assumed structure of the ${}^{11}\text{Li}$ wave function and that the effects are significant. Unfortunately, there are (at least) two problems that occur in attempts to validate this result by comparison with the existing experimental data. First of all, the Glauber-model calculations were shown to be highly sensitive to the core-target (i.e., ${}^9\text{Li}-{}^{12}\text{C}$) interaction, and there exists no independent determination of the ${}^9\text{Li} + {}^{12}\text{C}$ optical-model potential parameters. Thus, it was necessary to rely on extrapolations from elastic-scattering data obtained for nuclei of similar mass. In view of the strong sensitivity of the model to the core-target interaction (see Ref. [2], for example), this procedure is suspect.

The second problem that occurs in comparing elastic-scattering calculations with existing data is the inability of the experimental technique to resolve inelastic scattering to low-lying states of ${}^{12}\text{C}$, so that the data of Ref. [1] are actually for quasielastic scattering. In the ${}^{11}\text{Li} + {}^{12}\text{C}$ experiment inelastic excitation of ${}^{11}\text{Li}$ does not pose a problem, since there are no particle-stable excited states in this nucleus and the ${}^{11}\text{Li}$ projectile was detected and identified. In the ${}^9\text{Li} + {}^{12}\text{C}$ experiment, however, contributions due to inelastic excitation of the projectile do need to be considered. The excitation of the ${}^{12}\text{C}$ target was dealt with in Refs. [1] and [2] by calculating the inelastic contributions in either a coupled-

channel [1] or distorted-wave Born approximation (DWBA) [2] approach. While this is likely to be a reasonably accurate procedure, since the deformation of ${}^{12}\text{C}$ is well known, it nevertheless introduces some uncertainty into the comparison between theory and experiment.

The present experiment was designed to remedy the first of these two problems by measuring the ${}^9\text{Li} + {}^{12}\text{C}$ quasielastic angular distribution at the same incident energy per nucleon as for ${}^{11}\text{Li} + {}^{12}\text{C}$ in Ref. [1]. The velocity of the ${}^9\text{Li}$ (core or projectile) is then the same in the two experiments.

II. EXPERIMENTAL METHOD

The experimental setup is discussed in detail in Ref. [3]. In brief, we utilized three Si-CsI telescopes covering the range from 0° to 10° laboratory angle. Each telescope consisted of a $300\ \mu\text{m}$ thick by 5 cm square Si ΔE detector, a $300\ \mu\text{m}$ thick by 5 cm square double-sided (xy) silicon strip detector having 16 strips in each direction, and a CsI stopping detector with photodiode readout. The additional ΔE detector (not used in the setup described in Ref. [1]) gave improved separation of ${}^8\text{Li}$ from ${}^9\text{Li}$. The incident particles were tracked onto the target using two x - y position sensitive parallel plate avalanche counters separated by 1 m. The angular resolution was 0.25° full width at half maximum (FWHM) in the 1° – 4° telescope and 0.48° FWHM in the 3° – 10° telescope, including the uncertainty in the incident particle direction, the pixel resolution of the Si strip detector, and multiple scattering in the $592\ \text{mg}/\text{cm}^2$ natural C target. The beam energy was determined on an event-by-event basis using a thin plastic scintillator placed at the entrance to the scattering chamber. This detector allowed us to measure the time of flight of each incident particle over a distance of 40

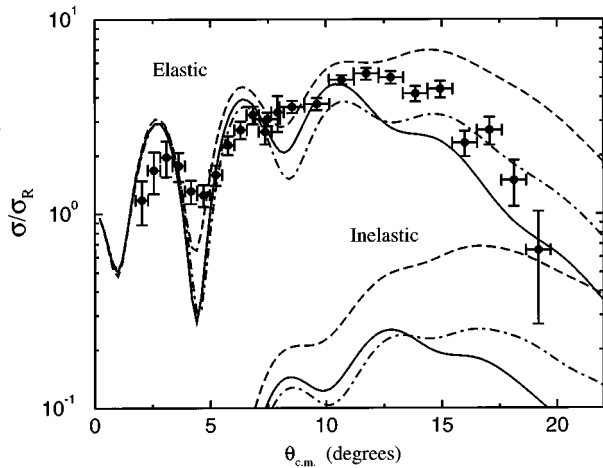


FIG. 1. Calculated ${}^9\text{Li}$ - ${}^{12}\text{C}$ elastic cross section angular distributions (ratio to Rutherford) using optical potential sets A (dashed curve), B (dot-dashed curve), and C (solid curve) are compared with the quasielastic data at 540 MeV. The DWBA cross sections for the inelastic excitation of ${}^9\text{Li}(1/2^-)$, 2.29 MeV, calculated using the three potentials, are also shown.

m from the A1200 fragment separator at Michigan State University which supplied the ${}^9\text{Li}$ secondary beam. In this way, we were able to improve the energy resolution of the experiment to 1.5% FWHM, compared with 7%–10% in Ref. [1]. The better resolution helped in the identification of the recoil ion, but was still insufficient to allow for the separation of “true” elastic scattering. Therefore, we again measured the quasielastic-scattering angular distribution including, in this case, excitation of both the ${}^9\text{Li}$ and ${}^{12}\text{C}$ systems. The incident particle rate was kept in the range from 500 to 1000 particles per second during the course of the experiment to eliminate problems due to pileup of the detected scattering events.

The ${}^9\text{Li}$ - ${}^{12}\text{C}$ quasielastic-scattering angular distribution measured in this experiment is shown in Fig. 1. The vertical error bars include both the statistical error and an estimate of the systematic uncertainty due to the angular resolution of the detector, indicated by the horizontal error bars.

III. CALCULATIONS OF ${}^9\text{Li}$ AND ${}^{11}\text{Li}$ SCATTERING

In the few-body Glauber model calculations of ${}^{11}\text{Li}$ scattering of Ref. [2], the core- (${}^9\text{Li}$) target (${}^{12}\text{C}$) effective interaction (optical potential) is a necessary theoretical and empirical input. In the absence of experimental data for ${}^9\text{Li}$ scattering in that study, three choices of distorting potential parameter sets were assumed in the core-target partition. These sets, obtained from a consideration of the potential descriptions of ${}^{12}\text{C}+{}^{12}\text{C}$ elastic scattering data (sets A and B) and suggested by a global parametrization of the optical potential for the lighter lithium isotopes (set C), were as follows:

$$\text{potential A: } V=140.0 \text{ MeV, } r_V=0.700 \text{ fm,}$$

$$a_V=0.900 \text{ fm, } W=25.00 \text{ MeV, } r_W=0.980 \text{ fm,}$$

$$a_W=0.750 \text{ fm;}$$

$$\text{potential B: } V=147.0 \text{ MeV, } r_V=0.641 \text{ fm,}$$

$$a_V=0.885 \text{ fm, } W=25.00 \text{ MeV, } r_W=1.012 \text{ fm,}$$

$$a_W=0.755 \text{ fm;}$$

$$\text{potential C: } V=122.3 \text{ MeV, } r_V=0.670 \text{ fm,}$$

$$a_V=0.930 \text{ fm, } W=18.46 \text{ MeV, } r_W=1.120 \text{ fm,}$$

$$a_W=0.700 \text{ fm.}$$

In all cases the potentials have volume real and imaginary Woods-Saxon terms and the radius parameters are multiplied by $9^{1/3}+12^{1/3}$.

In [2] these potentials were understood to be bare ${}^9\text{Li}$ - ${}^{12}\text{C}$ optical potentials which should describe ${}^9\text{Li}$ elastic scattering. Thus contributions to the ${}^{11}\text{Li}$ cross section from the inelastic excitation of the ${}^{12}\text{C}$ target, by the core and valence nucleons, were added explicitly, in the DWBA, to the calculated elastic cross sections to compare the calculations with the quasielastic data for the ${}^{11}\text{Li}$ - ${}^{12}\text{C}$ system at 637 MeV [1]. The calculated ${}^{11}\text{Li}$ cross section angular distributions [2] showed significant sensitivity to this central core-target interaction. We first investigate the extent to which these assumptions, and hence the results calculated in this earlier analysis, are confirmed by the quasielastic-scattering data for the ${}^9\text{Li}$ - ${}^{12}\text{C}$ system at 540 MeV presented here.

Figure 1 compares the calculated ${}^9\text{Li}$ - ${}^{12}\text{C}$ elastic cross section angular distributions (ratio to Rutherford) with the quasielastic data when using optical potential sets A (dashed curve), B (dot-dashed curve), and C (solid curve). Unlike the ${}^{11}\text{Li}$ - ${}^{12}\text{C}$ situation, the small angle behavior of the calculations follows the oscillatory trends and phase of the experimental data. Also evident is that the elastic cross sections calculated using the two potentials based on the ${}^{12}\text{C}$ - ${}^{12}\text{C}$ interaction (sets A and B) already exceed the quasielastic data for ${}^9\text{Li}$ at larger angles. It appears therefore that these core potentials, as used in [2], should be thought of as effective interactions which already include significant effects due to target excitation, which are included in the data.

The presented quasielastic data for the ${}^9\text{Li}$ - ${}^{12}\text{C}$ system also include contributions due to the inelastic excitation of ${}^9\text{Li}$. These effects should not be present in the ${}^9\text{Li}$ - ${}^{12}\text{C}$ interaction used as input to the few-body calculations of [2] for the ${}^{11}\text{Li}$ -target system. We estimate the likely importance of these effects by performing DWBA calculations of the cross sections for the inelastic excitation of the $1/2^-$ state of ${}^9\text{Li}$ at 2.69 MeV. The calculations are carried out assuming the $3/2^-$ and $1/2^-$ states of ${}^9\text{Li}$ lie in a $K=1/2$ rotational band and use a ${}^9\text{Li}$ deformation parameter $\beta=0.6$, deduced from the ground state quadrupole moment using the method detailed in [4]. The calculated inelastic cross sections, when using potentials A, B, and C above, are also shown in Fig. 1, where the curves have the same meaning as for the corresponding elastic calculations. In all cases the inelastic cross sections are smaller than those of the elastic channel by at least an order of magnitude and thus do not represent a serious uncertainty in the deduced ${}^9\text{Li}$ - ${}^{12}\text{C}$ interactions.

While the error bars on the present data do not permit a serious parameter search, making a relatively minor change

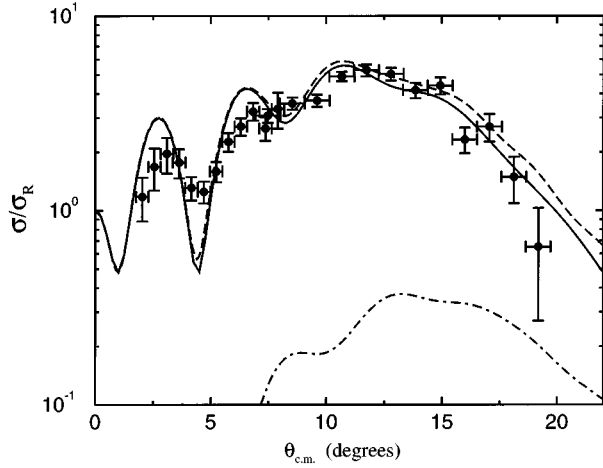


FIG. 2. Calculated ${}^9\text{Li}$ - ${}^{12}\text{C}$ elastic cross section angular distribution (ratio to Rutherford) using optical potential set D (solid curve) is compared with the quasielastic data at 540 MeV. The DWBA cross section for the inelastic excitation of ${}^9\text{Li}(1/2^-, 2.29 \text{ MeV})$, calculated using potential D, is shown by the dot-dashed line. The dashed line represents the sum of these elastic and inelastic cross sections.

in the real potential depth of potential set A, from 140 MeV to 120 MeV, leads to a significant improvement in the description of the data. The resulting elastic cross section obtained with this potential, set D,

$$\begin{aligned} \text{potential D: } V &= 120.0 \text{ MeV}, & r_V &= 0.700 \text{ fm}, \\ a_V &= 0.900 \text{ fm}, & W &= 25.00 \text{ MeV}, & r_W &= 0.980 \text{ fm}, \\ & & a_W &= 0.750 \text{ fm}, \end{aligned}$$

is presented in Fig. 2 by the solid curve. Also shown, by the dot-dashed curve, is the expected contribution due to inelastic excitation of the $1/2^-$ state of ${}^9\text{Li}$. The sum of the elastic and inelastic cross sections is shown by the dashed curve. The cross section calculated using potential set D, with or without the addition of the ${}^9\text{Li}$ inelastic contribution, generates a reasonable description of the quasielastic since contributions due to ${}^9\text{Li}$ excitation are small. Potential D will therefore be used as an effective ${}^9\text{Li}$ - ${}^{12}\text{C}$ interaction without further adjustment.

This effective interaction, when incorporated in calculations of ${}^{11}\text{Li}$ scattering, already includes to a good approximation the effects of target excitation due to the ${}^9\text{Li}$ core. When using this potential one must not therefore include explicit additional target excitation contributions due to the core, as was done previously.

Since ${}^9\text{Li}$ has spin $I=3/2$, the ${}^9\text{Li}$ optical potential may also contain a spin-orbit ($\vec{L} \cdot \vec{I}$) interaction or spin dependence of higher rank, such as a rank-2 tensor T_R interaction arising from the ${}^9\text{Li}$ projectile deformation. Since the relevant matrix elements of $\vec{L} \cdot \vec{I}$ increase with projectile energy and mass (i.e., the grazing L values) whereas those of the T_R operator involve a ratio of L values and are effectively constant with energy, spin-orbit terms are expected to be the dominant spin dependence at the energy of interest. We write

$$U_9(R) = U_9^{\text{cent}}(R) + U_9^{s.o.}(R) \vec{L} \cdot \vec{I}. \quad (1)$$

Spin-orbit terms were not considered in the analysis of ${}^{11}\text{Li}$ scattering in [2] where they could arise from both a core spin-orbit interaction or dynamically. We consider a simple model for the ${}^9\text{Li}$ -target spin-orbit term estimated assuming that its spin is due to an unpaired $p_{3/2}$ valence proton. The proton-target spin-orbit interaction $V_p^{s.o.}(r_p) \vec{\ell}_p \cdot \vec{s}_p$ is then folded over the assumed $p_{3/2}$ configuration Φ_I ,

$$\Phi_{IM_I}(\vec{r}) = \phi_{\ell}(r) \sum_{m, \sigma_p} (\ell m s_p \sigma_p | IM_I) Y_{\ell m}(\hat{r}) \chi_{s_p \sigma_p}, \quad (2)$$

with ϕ_{ℓ} the proton radial wave function and $\chi_{s_p \sigma_p}$ its spinor. Thus

$$U_9^{s.o.}(R) \vec{L} \cdot \vec{I} = \langle \Phi_I | V_p^{s.o.}(r_p) \vec{\ell}_p \cdot \vec{s}_p | \Phi_I \rangle, \quad (3)$$

where, following [5], the potential form factor is

$$\begin{aligned} U_9^{s.o.}(R) = \int_0^{\infty} r^2 dr \phi_{\ell}^2(r) & \left[\frac{\gamma_1}{3} v_0^{s.o.}(r, R) + \frac{\gamma_1}{15} v_2^{s.o.}(r, R) \right. \\ & \left. + \frac{2\gamma_2}{5} \frac{r}{R} v_1^{s.o.}(r, R) \right]. \end{aligned} \quad (4)$$

For the ${}^9\text{Li}$ - ${}^{12}\text{C}$ system $\gamma_1 = (12+9)/[9(12+1)] = 7/39$ and $\gamma_2 = 8\gamma_1/9$ [6]. The multipole components of the proton spin-orbit interaction are

$$v_k^{s.o.}(r, R) = \frac{1}{2} \int_{-1}^1 V_p^{s.o.} \left(\left| \vec{R} + \frac{8}{9} \vec{r} \right| \right) P_k(\mu) d\mu, \quad (5)$$

with $\mu = \hat{r} \cdot \hat{R}$.

To obtain a quantitative estimate of this static spin-orbit component we assume the geometry for $V_p^{s.o.}(r_p)$ of Becchetti and Greenlees [7] and further assume that ϕ_{ℓ} ($\ell=1$) is described by a p -wave oscillator single particle state of length parameter a . Explicitly,

$$\phi_1(r) = N_1 r \exp(-r^2/[2a^2]), \quad N_1 = 2(4[9\pi a^{10}])^{1/4}. \quad (6)$$

The curves in Fig. 3 show the calculated ${}^9\text{Li}$ - ${}^{12}\text{C}$ spin-orbit potential form factors when using oscillator parameters $a=1.50 \text{ fm}$ (solid curve) and $a=1.77 \text{ fm}$ (dashed curve) for the bound proton and are of volume form. Inclusion of these spin-orbit terms introduces negligible changes in the calculated ${}^9\text{Li}$ - ${}^{12}\text{C}$ cross sections. Small effects arise only when the spin-orbit strength is scaled by an order of magnitude. Similar conclusions regarding uncertainties due to spin-orbit terms were recently reached by Satchler [8] in the context of heavier systems and within the double folding model. While additional surface spin dependence can arise from dynamical coupling [5], these effects fall with increasing energy. We do not consider spin-dependent terms further at present.

In summary, the measured quasielastic-scattering angular distribution for ${}^9\text{Li}$ - ${}^{12}\text{C}$ at 540 MeV is reproduced by a conventional volume form potential parametrization. Potential set D above provides a reasonable description of the quasielastic data without resort to the addition of explicit contri-

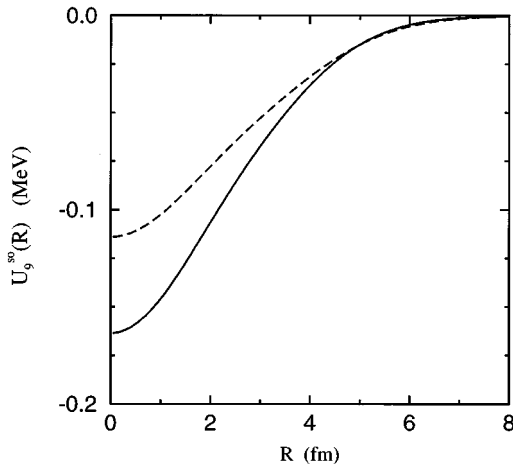


FIG. 3. Calculated ${}^9\text{Li}$ - ${}^{12}\text{C}$ spin-orbit potential form factors when using oscillator parameters $a=1.50$ fm (solid curve) and $a=1.77$ fm (dashed curve) for the bound proton.

contributions due to target excitation channels. Contributions to this quasielastic cross section due to ${}^9\text{Li}$ inelastic excitation are shown to be small. Potential D and those used in the earlier analysis of ${}^{11}\text{Li}$ scattering [2] should therefore be regarded as effective interactions, and not bare optical potentials. The new data presented show that these interactions already include the dominant effects of target excitation due to the core. When used as input to few-body models of the ${}^{11}\text{Li}$ - ${}^{12}\text{C}$ system, and calculating the quasielastic cross section for this composite system, one should not therefore add explicitly additional target excitation contributions, unless those contributions due to the valence nucleons can be delineated in some way.

Figure 4 compares the experimental [1] and calculated ${}^{11}\text{Li}$ - ${}^{12}\text{C}$ quasielastic cross section angular distributions (ratio to Rutherford) at 637 MeV. The solid curve is calculated using the four-body Glauber model of Ref. [2]. The ${}^{11}\text{Li}$ structure input to this calculation is the representative $O(7)$ three-body wave function for ${}^{11}\text{Li}$ used in Ref. [2] and described more fully in Ref. [9], in which the valence neutrons are assumed to be in a $(0p_{1/2})^2$ configuration. Potential D is used for the ${}^9\text{Li}$ -target interaction. The neutron-target optical potential is given by the global Becchetti-Greenlees parametrization [7] with the parameters used in Ref. [2]. Cross sections for target inelastic excitation have not been added to the elastic cross section. The well-documented small angle discrepancy with the data remains. However, the larger angle data are well described by the calculation.

IV. CONCLUSIONS

The ${}^9\text{Li} + {}^{12}\text{C}$ quasielastic-scattering angular distribution has been measured at an incident energy of 60 MeV per

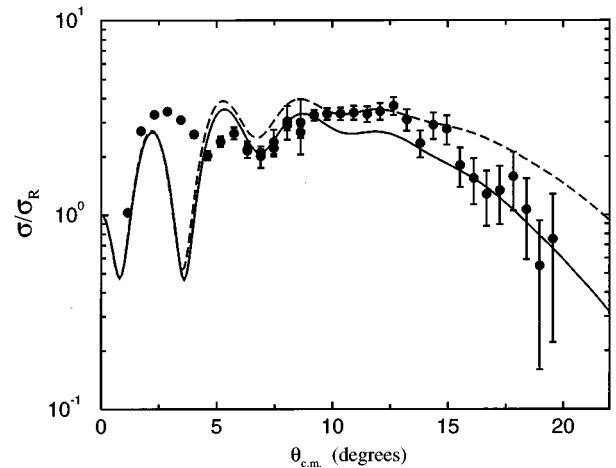


FIG. 4. Experimental and calculated ${}^{11}\text{Li}$ - ${}^{12}\text{C}$ cross section angular distributions (ratio to Rutherford) at 637 MeV. The solid curve is calculated using potential D as input to the four-body Glauber model. The dashed curve uses the original potential set A. The points are the quasielastic scattering data from [1].

nucleon. The differential cross section in the vicinity of the “rainbow peak” is about 70% greater than for ${}^{11}\text{Li} + {}^{12}\text{C}$, in agreement with the prediction that the dynamic polarization potential due to the extra two neutrons introduces increased absorption in the region of the nuclear surface. An effective potential, which produces a qualitatively good fit to the experimental data, has been derived. The corresponding parameter set is a slight modification of one used previously for calculations of ${}^{11}\text{Li} + {}^{12}\text{C}$ quasielastic scattering, but is now considered to include implicitly the effects of target excitation due to the ${}^9\text{Li}$ core. When used in a reanalysis of the ${}^{11}\text{Li}$ scattering, this effective potential produces a reasonable description of the experimental data at large angles without the need to add target inelastic cross section contributions. The main conclusions of Ref. [2], regarding the sensitivity of the ${}^{11}\text{Li}$ cross section to the different three-body wave functions for the projectile, remain valid. However, the availability of the new ${}^9\text{Li}$ data has removed a major ambiguity from the theoretical inputs to the four-body calculations of the ${}^{11}\text{Li} + {}^{12}\text{C}$ system.

ACKNOWLEDGMENTS

Support for this work was provided by the U.S. National Science Foundation under Grants Nos. PHY94-02761 and PHY92-14992, and by the U.S. Department of Energy under Contract No. W-31-109-ENG-38. The financial support of the Science and Engineering Research Council (U.K.) through Grants Nos. GR/J95867 and GR/K33026 is also acknowledged.

[1] J.J. Kolata, M. Zahar, R. Smith, K. Lamkin, M. Belbot, R. Tighe, B.M. Sherrill, N.A. Orr, J.S. Winfield, J.A. Winger, S.J. Yennello, G.R. Satchler, and A.H. Wuosmaa, Phys. Rev. Lett. **69**, 2631 (1992).

[2] I.J. Thompson, J.S. Al-Khalili, J.A. Tostevin, and J.M. Bang, Phys. Rev. C **47**, R1364 (1993); J.S. Al-Khalili, I.J. Thompson, and J.A. Tostevin, Nucl. Phys. **A581**, 331 (1995).

[3] M. Zahar, M. Belbot, J.J. Kolata, K. Lamkin, R. Thompson,

- J.H. Kelley, R.A. Kryger, D.J. Morrissey, N.A. Orr, B.M. Sherrill, J.S. Winfield, J.A. Winger, and A.H. Wuosmaa, Phys. Rev. C **49**, 1540 (1994).
- [4] F.M. Nunes, I.J. Thompson, and R.C. Johnson, Nucl. Phys. **A596**, 171 (1996).
- [5] H. Nishioka, J.A. Tostevin, R.C. Johnson, and K.-I. Kubo, Nucl. Phys. **A415**, 230 (1984).
- [6] It should be noted that the core-valence particle position vector \vec{r} used here is opposite to that of [5].
- [7] F.D. Becchetti and G.W. Greenlees, Phys. Rev. **182**, 1190 (1969).
- [8] G.R. Satchler, Nucl. Phys. **A579**, 341 (1994).
- [9] J.M. Bang and I.J. Thompson, Phys. Lett. B **279**, 201 (1992).